AAS 14-273

A CONTINUATION METHOD FOR CONVERTING TRAJECTORIES FROM PATCHED CONICS TO FULL GRAVITY MODELS

Nicholas Bradley*, and Ryan P. Russell†

A method is introduced to transition space trajectories from low fidelity patched conics models to full-ephemeris n-body dynamics. The algorithm incorporates a continuation method that progressively re-converges solution trajectories in systems with incrementally higher fidelities. Continuation is accomplished through the variation of a control parameter, which is tied to body parameters such as ephemerides, mass, minimum flyby altitude, and sphere of influence size. The intermediate models provide a continuous and differentiable path between solutions in the simplified and n-body dynamics. Each successive step preserves the individual flyby properties by altering periapsis flyby states and body masses, ensuring that the final converged solution is qualitatively similar to the initial guess. A similar approach to this methodology may be taken with any simplified starting guess, such as a restricted three-body model. Trajectories computed using the patched conics conversion method presented here may include gravity assists and rendezvous with any number of target bodies, so the method is ideal for constructing interplanetary or intermoon tour missions.

INTRODUCTION

In the field of orbital mechanics, it is common to approximate interplanetary trajectories in low fidelity models that assume simplified system dynamics. Some notable assumptions are the patched conics model using two-body dynamics, or a restricted three-body model. Trajectories in these reduced models are ideal for rapid searches and fundamental understanding of broad preliminary design spaces. However, simplified models are not sufficient for cases where the model assumptions are invalid, or when a preliminary design moves to a more advanced design stage.

Much of the literature on tour design incorporates only simplistic models, and often implies that the transition to higher fidelity models is a trivial process. Many authors have addressed ballistic patched conics tour design[1–3] (often with novel methods that are quite useful), but few have presented systematic algorithms for representing the results in n-body ephemeris models. Typically, the transition to the full ephemeris model is made in a single leap, and can stress even the best optimization algorithms tackling the simplest of problems.

Previously, the application of a "multi-conic method" with differential correction was explored by Wilson and Howell[4] with applications to the Sun-Earth-Moon environment. Their work is based on

*Ph.D. Candidate, Department of Aerospace Engineering and Engineering Mechanics, The University of Texas at Austin, W.R. Woolrich Laboratories, 1 University Station, C0600, 210 E. 24th St., Austin TX 78712, USA; Student member AIAA and AAS. nick.bradley@utexas.edu

†Assistant Professor, Department of Aerospace Engineering and Engineering Mechanics, The University of Texas at Austin, W.R. Woolrich Laboratories, 1 University Station, C0600, 210 E. 24th St., Austin TX 78712, USA; Member AIAA and AAS. ryan.russell@austin.utexas.edu

the original multi-conic method,[5] which approximates trajectory legs by considering separate perturbing influences. This method is somewhat of a compromise between patched conics and fully integrated trajectories. In another work, Marchand, Howell, and Wilson[6] utilized a multi-step correction process for obtaining trajectories in an n-body ephemeris model. This procedure begins with a "seed" trajectory, divides the trajectory into nodes, and performs differential correction on the states at the nodes to satisfy specified constraints in the n-body model. This method does not consider continuation, but relies on differential correction to converge trajectories in n-body ephemerides. Buffington and Strange[7] developed a method used for Cassini moon tours that differentially corrects the hyperbolic excess velocity to meet certain conditions, calling it the "patched-integrated" method.

For an Earth-to-Moon transfer, Griesemer, Ocampo, and Cooley[8] obtained an initial guess in a lower-fidelity three-body model, and used this guess as an initial condition for convergence in a higher-fidelity model, but without considering any intermediate solutions. In a very mathematical description, Picot[9] applies a continuation method to the low-thrust orbit transfer problem by iteratively solving the problem at different values of the control bound and retaining each solution for the successive initial guess.

Lantoine and Russell[10] utilized a continuation method to take trajectories in a patched three-body problem and converge them in a more realistic ephemeris-based four-body model. This method uses linear interpolation between two ephemerides, but does not continue trajectories to a n-body solar system trajectory model. Instead, the authors generate an auxiliary four-body ephemeris to more closely approximate the true system dynamics, but they do not include the n-body ephemerides in the final solution. Russell and Strange[11] make use of a continuation method to transition between a patched conics ideal model and a patched conics ephemeris model when searching for cycler trajectories in planetary moon systems by interpolating between two ephemerides. This approach is similar to the current study, but the patched conics ephemeris trajectories are used directly as initial guesses in the n-body dynamical model without any continuation process. Russell and Ocampo[12] utilized a continuation architecture to calculate cycler trajectories in n-body ephemeris models from basic circular coplanar models, but the solutions obtained are still in a patched conics framework.

Continuation methods have been applied to spacecraft trajectories previously for the purpose of determining orbit families and solution bifurcations. Biggs and McInnes[13] computed families of solar sail orbits about the Earth-Moon L_1 point by using the solar sail angle as the continuation parameter. Chow and Villac[14] determined families of periodic orbits and optimal spacecraft placements along periodic orbits in the Earth-Moon system via a continuation method. Paffenroth, Doedel, and Dichmann[15] used numerical continuation to generate families of periodic orbits about the Earth-Moon L_1 point, and their work provides a good mathematical summary of continuation methodology in general. Yagasaki[16] obtained Δv-optimal trajectories in the Earth-Moon three-body problem by using continuation methods on an initial seed transfer trajectory. Casoliva et. al.[17] used a continuation method for multiple applications to calculate and classify Earth-Moon cycler trajectories. Their work includes a method of determining resonant transfers by continuing the system mass parameter μ from small to large values, and also determines families of cyclers by continuing the Jacobi constant in the three-body model.

Here, a method is proposed to take a given low fidelity trajectory and obtain a trajectory in an n-body ephemeris with actual body masses via continuation on mass and ephemeris parameters. The resultant trajectory is subject to the same constraints as in the simplified problem. The goal is accomplished via continuation on a control parameter $\kappa \in [0, 1]$ that is incremented in steps

to represent an increasingly more complex dynamical model. Between each step, the flyby radii, body masses, and sphere of influence sizes are artificially altered such that the turning angles and flyby properties from the previous converged solution are preserved. This preservation is illustrated schematically in Figure 1. Additionally, the body ephemerides vary linearly with κ from purely two-body Keplerian ephemerides ($\kappa = 0$) to n-body ephemerides ($\kappa = 1$). The converged solution at each value of the control parameter is continuous with fully-defined ephemeris states for all bodies, and the transition between ephemerides is smooth. Individual body masses are also tied to the control parameter so that perturbative gravitational effects increase from a two-body to an n-body model. Eventually, at $\kappa = 1$, the driving model coincides with the n-body ephemeris model, and a converged trajectory in this system represents a purely ballistic trajectory that satisfies interior continuity constraints.

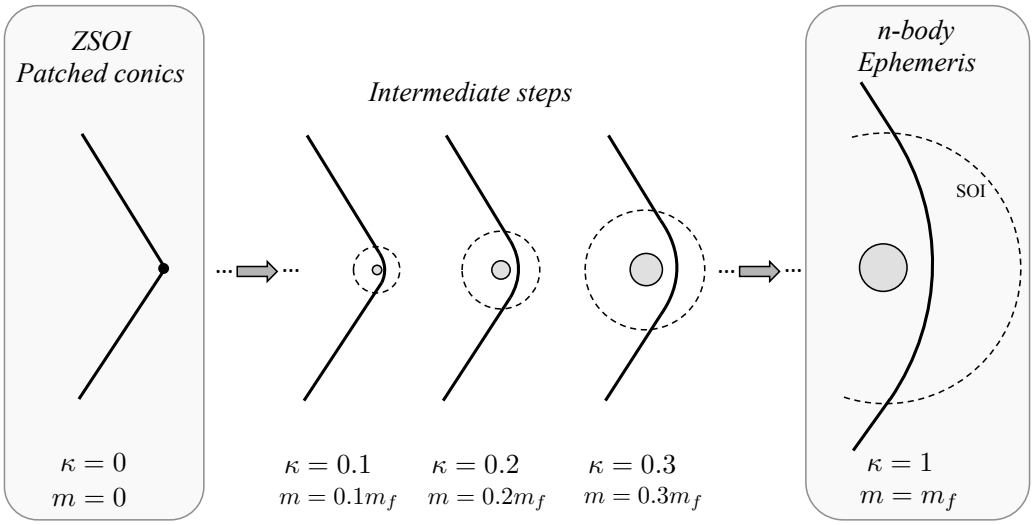

Figure 1: Schematic of the continuation method preserving flyby geometry and turning angle

As a broad summary of the current work, there exists an "outer loop," which is comprised of the continuation method and the calculation of an auxiliary "fake" ephemeris, and an "inner loop," which contains the specific solution method for each step of the continuation. This inner loop may be any solution method to converge feasible trajectories. In the current work, execution of the inner loop is accomplished by altering the close approach flyby states to satisfy continuity constraints in an optimization algorithm.

The first section outlines the overview of the algorithm, and gives a pseudo-algorithm of how to convert a given "zero sphere of influence" (ZSOI) trajectory into actual n-body dynamics. The method described in this work is applicable to any simplified starting model; the ZSOI model is chosen because it is the preliminary starting point for many mission designers. The details begin with the following section, describing the auxiliary Keplerian ephemerides, which is a Keplerian version of the n-body ephemerides for the target bodies. The purpose of the Keplerian ephemerides is to facilitate the definition of a continuous set of "fake" ephemerides for each intermediate step in the continuation method. A brief differential correction procedure is then described to transfer an initial ZSOI trajectory into these new Keplerian ephemerides. The process of finding an initial feasible solution using an optimization algorithm is described next. The continuation method, which

utilizes the feasible solution process for increasingly realistic dynamical systems, is developed next. Two examples are given: one of a simple Ganymede to Callisto transfer about Jupiter, and one of a more complex Earth-Venus-Venus-Earth-Jupiter ballistic transfer. Finally, some concluding remarks are presented.

ALGORITHM OVERVIEW

The final goal of the algorithm is to converge a spacecraft trajectory in an n-body dynamical ephemeris (e.g. JPL's SPICE ephemerides[i]), with dynamics governed by bodies of actual mass and size (as opposed to a massless or point-mass assumption). It is assumed that the user has an initial trajectory in a ZSOI model, which can be either in a full ephemeris system or in a simplified ephemeris system.

The "outer loop" of the continuation method operates by conducting a smooth transition between dynamical models and mass assumptions. In this algorithm, parameters of body mass, sphere of influence size, and body ephemerides are varied by the control parameter κ. The goal is to achieve a smooth transition between the starting (simplified) dynamics and the desired final dynamics.

The first step is to create a set of mean Keplerian ephemerides for the desired bodies over the timespan of interest. The motivation behind this auxiliary ephemeris set is described in the following section. Next, the initial trajectory (whether it uses "real" ephemerides or some other assumed ephemeris model) is reconverged in the Keplerian ephemerides. These ephemerides closely approximate the final "real" ephemerides of the bodies, so the transition between these two ZSOI models is accomplished in a relatively simple manner. Finally, with a converged trajectory in the Keplerian ephemerides, the "outer loop" continuation method begins, and the body properties of mass, ephemeris, and sphere of influence size are all altered until convergence in the final n-body dynamical system is obtained.

These steps are all outlined in Algorithm 1, and described in detail in the subsequent sections.

Algorithm 1 Overview of steps to converge a trajectory in full n-body dynamics

Require: A desired final ephemeris set
Require: An initial ZSOI trajectory in some ephemeris model
1: Create a mean Keplerian ephemeris for all bodies over the timespan of interest
2: **if** Initial trajectory is not Keplerian ephemerides **then**
3: Perform differential correction on flyby times to converge trajectory in Keplerian ephemerides
4: **end if**
5: Initialize $\kappa < 1$ to begin continuation
6: Set a $\Delta\kappa$ appropriate for the problem in question
7: **while** $\kappa \leq 1$ **do**
8: Update current guess of flyby states based on κ to preserve flyby parameters
9: Converge trajectory in new dynamics using "inner loop"; may be optimization or other method
10: Increment: $\kappa = \kappa + \Delta\kappa$
11: **end while**
12: Final converged solution is in n-body full ephemeris dynamics

[i]The SPICE toolkit, data, and documentation may be accessed on-line at: http://naif.jpl.nasa.gov/naif/

THE AUXILIARY EPHEMERIDES

The "real" ephemerides represented by an n-body dynamical model are produced in a non-Keplerian framework, and the final resulting spacecraft trajectory is subject to the same dynamical environment. However, if the procedure is to begin with a ZSOI model, the initial guess should be propagated in a corresponding dynamical environment. This dynamical consistency between the forces affecting the spacecraft and the target bodies leads to a smoother targeting or optimization problem, improving robustness and the likelihood of convergence. To achieve such consistency, an auxiliary Keplerian ephemeris is created that is subject to the same two-body dynamical assumptions as a ZSOI spacecraft in a "real" ephemeris model. This Keplerian ephemeris must be chosen to closely approximate the real ephemerides that are governed by the dynamics of the n-body system. Ephemerides at any step in the continuation process are called "fake" ephemerides, and are related to the control parameter κ according to Eq. (1), where $\mathbf{x}$ represents the state vector $[\mathbf{r}, \mathbf{v}]^\top$.

$$\mathbf{x}_{fake}(\kappa) = (1-\kappa)\mathbf{x}_{kepler} + \kappa\mathbf{x}_{real} \tag{1}$$

The benefit of this auxiliary ephemeris is clearly seen by examining the trajectory of a spacecraft with respect a target body. Take, for example, a spacecraft that performs a "backflip" (or half-revolution resonance) trajectory with the Earth, departing Earth at some time and returning half a year later. One may determine the ephemeris state of the Earth in two different ephemeris models: a "real" ephemeris model (e.g. SPICE), and an auxiliary "Keplerian" ephemeris model that is subject only to heliocentric two-body dynamics. Generating a simple backflip trajectory in both the real and Keplerian ephemeris models and subtracting the ephemeris position of the Earth with respect to the Sun yields an Earth-centered trajectory in each ephemeris model.

It is expected that a valid backflip trajectory in an Earth-centered inertial frame be smooth, and that it begins and ends at the origin. Only by targeting the Keplerian Earth and performing the origin offset with the Keplerian ephemeris is the expected result realized. Other ephemeris combinations for targeting and offset yield results that do not agree with the expectations.

Figure 2 shows a grid of trajectories that target the real or Keplerian ephemeris, and perform the origin offset with a real or Keplerian ephemeris. Subfigure (a) is real/real, (b) is real/Keplerian, (c) is Keplerian/real, and (d) is Keplerian/Keplerian.

The wavy nature of subfigure (a) is due to the discrepancy in dynamical models. Because the spacecraft state (propagated in the two-body model) is offset by the real Earth position, the resultant relative position reflects the fact that the real Earth is affected by dynamics that are not taken into account by the ZSOI model. Additionally, the spacecraft does not return to the origin at the final time. Although an origin offset using the Keplerian ephemeris (b) creates a smooth trajectory, the endpoint states of the Earth are still different between the two ephemeris models, and so the spacecraft still does not return to the origin. The real ephemeris offset targeting a Keplerian Earth in (c) suffers from the same problem as in (b): the endpoints are different between the two ephemeris models, and so the spacecraft does not return exactly to the origin. The waviness is also present here as an artifact of the dynamical model differences between the ephemerides.

Only by obtaining the Earth's positions in a Keplerian ephemeris and using that same Keplerian ephemeris to offset the origin to the Earth is the desired result obtained (d). Using only the Keplerian ephemeris yields smooth results, which is desirable for favorable convergence characteristics in gradient-based optimization methods. Using mismatched ephemerides can lead to inaccurate so-

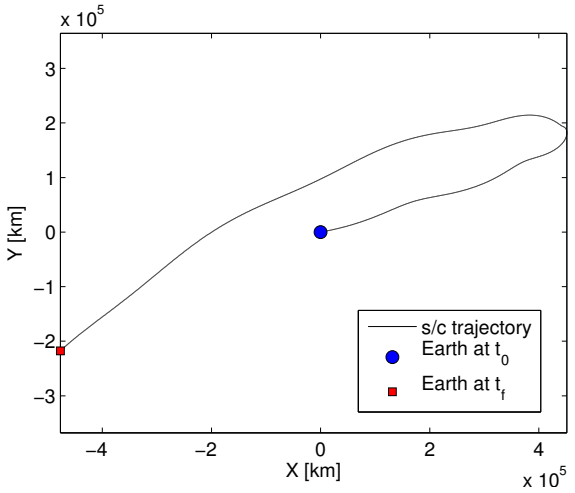

(a) Spacecraft position targeting real Earth ephemerides. Position corrected with real Earth ephemerides.

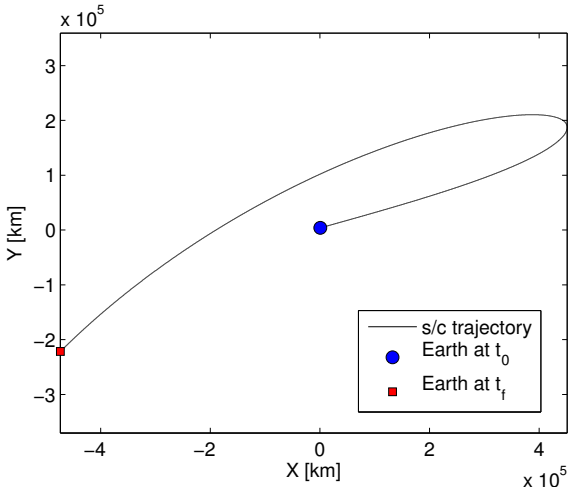

(b) Spacecraft position targeting real Earth ephemerides. Position corrected with Keplerian Earth ephemerides.

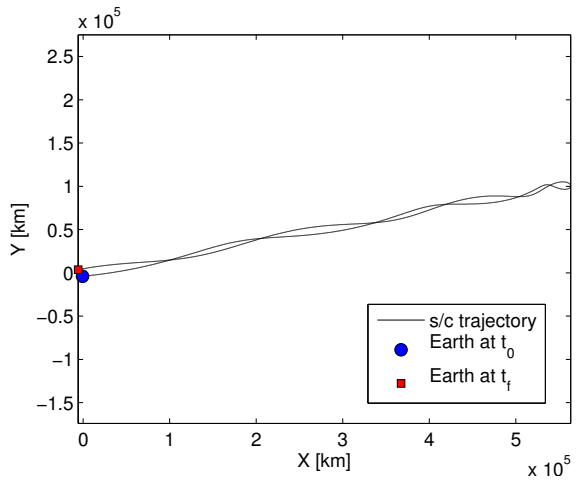

(c) Spacecraft position targeting Keplerian Earth ephemerides. Position corrected with real Earth ephemerides.

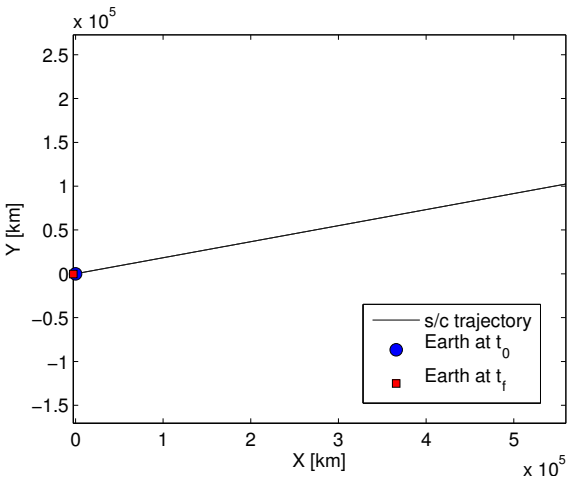

(d) Spacecraft position targeting Keplerian Earth ephemerides. Position corrected with Keplerian Earth ephemerides.

Figure 2: Geocentric representation of heliocentric trajectory using Earth positions in different ephemerides for origin offset

lutions, and can prevent an optimization or targeting algorithm from converging on a solution at all.

Keplerian ephemeris generation

It is beneficial, therefore, to create an ephemeris that represents the target bodies' states (B) about the central body (A) in the ZSOI model, but that approximates the real n-body ephemerides closely. This ephemeris generation is accomplished in two steps: a geometric generation to obtain a close

approximation of the desired trajectory, and a least squares correction to ensure close ephemeris matching.

Geometric generation Over a time period of interest, say t_0 to t_f, and at a time interval dt, SPICE is queried to obtain the actual ephemeris state of B with respect to A over the time span. At each queried time, the ephemeris state is converted to Keplerian orbital elements through a standard routine. For n distinct times in the range $[t_0, t_f]$, there are n distinct osculating values for each orbital element (a, e, i, Ω, ω, and ν). Because the desired ephemeris represents a two-body Keplerian orbit of B about A, there may only be one constant value of each of the first five orbital elements.

It is especially important to match the mean motion of B about A, so taking the mean of the semimajor axis values will not reliably generate a Keplerian ephemeris that is close enough to the real ephemeris. To obtain a satisfactory value for a, the angular motion of the real ephemeris state of B is accumulated throughout the time period of interest. At each time step, the angle is calculated between the position vector and and a reference axis in the osculating orbital plane at t_0. At the end of the time period, the mean motion is calculated from the full accumulated angle. The relevant steps are summarized in Algorithm 2.

Algorithm 2 Determining mean motion for the Keplerian ephemerides

1: Initialize $m = 0$
2: At t_0, calculate θ_0, the angle between $\mathbf{r}_0$ and the reference axis in the perifocal frame.
3: **for all** $t_0 < t \leq t_f$ **do**
4: Calculate θ, the angle between $\mathbf{r}$ and the reference axis.
5: **if** $\theta_{i-1} < \theta_0$ **and** $\theta_i > \theta_0$ **then**
6: Increment $m = m + 1$
7: **end if**
8: **end for**
9: At t_f, calculate the angle α between $\mathbf{r}_0$ and $\mathbf{r}_f$, taking care to account for quadrant issues for the possibility of an angle $\pi < \alpha < 2\pi$.
10: Finally, calculate the full angle traversed over the timespan as $\Theta = 2\pi m + \alpha$.
11: Calculate the mean motion from the full angle traversed (Eq. (2)).

The mean motion may be obtained as the total traversed angle divided by the total timespan:

$$n_B = \frac{\Theta}{t_f - t_0} \tag{2}$$

From this equation, the semimajor axis that best represents the overall mean motion of B about A is found as:

$$a_B = \left[\frac{\mu_A}{n_B^2}\right]^{1/3} \tag{3}$$

The next four orbital elements may be reasonably found as the mean of their osculating values throughout the time period. Any error this introduces, especially in Ω and ω, is corrected in the least squares procedure in the following subsection.

$$e_B = \text{mean}(e), \quad i_B = \text{mean}(i), \quad \Omega_B = \text{mean}(\Omega), \quad \omega_B = \text{mean}(\omega) \tag{4}$$

Finally, the true anomaly at t_0 must be found to complete the orbital element set, which leads to a completed Keplerian ephemeris. Since all other orbital elements have been defined, there now exists a true perifocal frame which entirely contains the Keplerian orbit. The initial true anomaly, $\nu_{B,0}$, is found as the angle between the projection of $\mathbf{r}_0$ on this perifocal frame and the perifocal frame $+X$ axis, which points toward periapsis.

$$\nu_{B,0} = \cos^{-1}\left(\frac{\mathbf{r}_0 \cdot X}{|\mathbf{r}_0|}\right) \tag{5}$$

The result of Eq. (5) must be appropriately checked for necessary quadrant corrections.

This algorithm results in the six Keplerian orbital elements which define a Keplerian two-body ephemeris. This result is converted to a Cartesian state at the initial time, and a least squares correction algorithm is applied to this initial vector to ensure a close match between the real and Keplerian ephemerides.

Least squares correction The initial state $\mathbf{X}_0 = [\mathbf{r}_0, \mathbf{v}_0]^\top$ is iteratively corrected from the geometric guess to minimize the sum of the squares of the distances between the positions of the two ephemerides at equally-spaced times throughout the defined time span of interest. This correction is accomplished by using a batch correction algorithm,[18] which is common in estimation problems. In short, the initial state is propagated in the two-body model to the times of interest along with the state transition matrix $\mathbf{\Phi}$. Denoting the real ephemeris values as the "observations" and the propagated states as the "computed" values, an error vector $\mathbf{y}$ is formed at time t:

$$\mathbf{y} = \mathbf{r}_{\text{real}}(t) - \mathbf{r}_{\text{kepler}}(t) \tag{6}$$

By using an iterative least squares correction with $\mathbf{\Phi}$, the error vector in Eq. (6) is minimized at each time step. This process involves iteration on the initial Cartesian state vector $\mathbf{X}_0$, and usually converges in a few steps since the initial guess from the geometric method is close. In a two-body sense, $\mathbf{X}_0$ fully defines the ephemeris, since ephemeris states may be obtained by simply propagating the initial state in a two-body model.

Ephemeris comparison

The real and Keplerian ephemerides may be compared by simple vector subtraction of the position throughout the time span of interest. Good ephemeris matching is shown by a constant (zero or non-zero) mean offset of position throughout the time span. The ephemeris matching steps are intended to obtain as close a match as possible, but due to dynamical differences between the models assumed in the two ephemerides, there is a non-zero offset that remains. Figure 3 demonstrates the ephemeris comparison for Ganymede and Callisto orbiting about Jupiter. The difference in position of each body about Jupiter over time oscillates between the two ephemerides, but there is no secular growth, indicating that the ephemerides (and, especially, the mean motions) are well-matched.

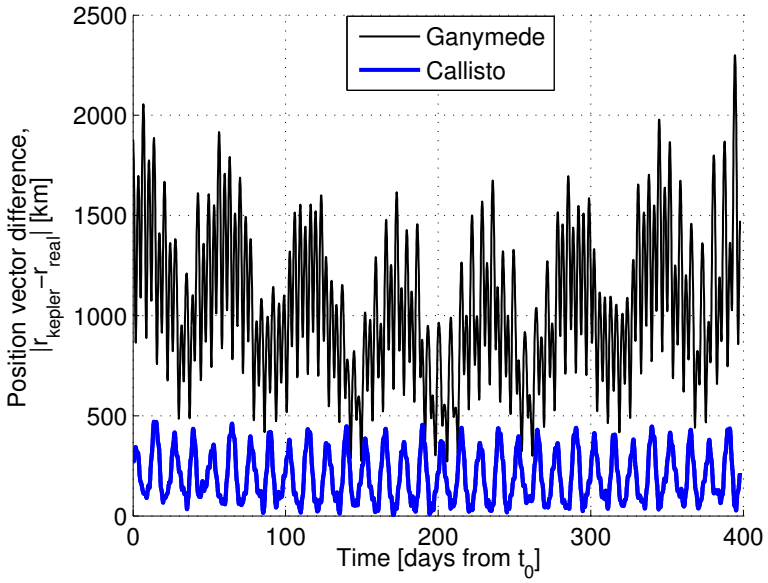

Figure 3: Variation in orbital position between the Keplerian and real ephemerides, demonstrating good ephemeris matching

DIFFERENTIAL CORRECTION FOR V_∞ MATCHING

If the initial ZSOI trajectory is in an ephemeris model other than the mean Keplerian ephemerides created in the previous section, then the trajectory must be re-converged in the new ephemerides (see Algorithm 1). Because the Keplerian ephemerides have been created to be very close to the full n-body ephemerides, the correction is small.

A simple differential correction scheme is utilized, where the intermediate body flyby times are differentially corrected to match interior v_∞ constraints. Matching is accomplished with a Newton-Raphson differential corrector, which is appropriate to use, given the assumption that the desired Keplerian ephemeris model is very close to an ephemeris model of the trajectory. For n bodies, there are $n-2$ parameters (the flyby times of the intermediate bodies, which does not include the initial and final bodies) and $n-2$ constraints, which are the matching v_∞ parameters at each intermediate body. Denote the flyby times as a vector $\mathbf{t}$, and the constraints as a vector $\mathbf{c}$, both of which are $(n-2)\times 1$ in size. (The values of $\mathbf{c}$ should be very small, given the assumption of the close matching of the ephemerides). Then, the differential correction proceeds iteratively according to Eq. (7). At each step of the correction, the trajectory is re-calculated between each body at the specified encounter times using Lambert targeting, which is described extensively in the literature (e.g., see Battin[19] and Vallado[20] for derivations and algorithms). Since the ephemeris model being used is a Keplerian ephemeris, this procedure is very amenable to using a Lambert targeting scheme because of the identical two-body assumptions in the ephemeris and the targeting.

$$\mathbf{t}_{i+1} = \mathbf{t}_i - \left[\frac{\partial \mathbf{c}}{\partial \mathbf{t}}\right]^{-1} \mathbf{c} \tag{7}$$

The correction proceeds until the constraints have all been matched to within a certain tolerance (which is set to 1 m/s in this work). In practice, this should take only a few iterations. The matrix

$[\partial \mathbf{c}/\partial \mathbf{t}]$ may be found by any partial derivative method, whether numerical or analytic. In this work, the matrix is calculated via a forward differencing numerical method.

Upon convergence of the Newton-Raphson scheme in Eq. (7), the user has a trajectory that is fully converged in a ZSOI Keplerian ephemeris system. The next step is to describe the method of finding a feasible solution in the intermediate models before defining the continuation method.

FINDING A FEASIBLE SOLUTION

To find a feasible solution in the n-body dynamics, one must find a feasible solution at each step of the continuation method (the "inner loop"). There are many suitable methods to find a feasible trajectory solution, or to converge a trajectory with some minimized cost function. In the current work, the desire is to find a feasible end-to-end ballistic trajectory with no deterministic maneuvers, continuous in position and velocity to within a certain tolerance. The approach is to vary the free parameters (states and times) to satisfy continuity constraints. This sub-algorithm comprises the inner loop, which is solved for each successive iteration of the outer loop continuation process. Although a specific procedure is presented here, any suitable solution method for the inner loop may be substituted.

In this solution approach, a multiple shooting method is used to break the trajectory into several segments. Because interbody trajectories often operate in regions with fast-changing dynamics that can greatly alter the final solution of the problem, it is common practice to separate the full trajectory into several segments and converge the solution with intermediate patch points.

Patch points

The patch points are defined by flight times from the close approach time at each target body. These flight times are intended to approximate the location of the sphere of influence of each body, but any time may be used that is sufficiently far away from the target body, yet not so far away that the patch state is highly sensitive to the flyby state at the close approach.

Define the radius of the sphere of influence as the commonly-used Eq. (8). Note that the gravitational parameter μ is multiplied by the control parameter κ. The quantity r_{AB} is the distance between the central body and the target body, and the subscripts A and B denote the central and target bodies, respectively.

$$r_{SOI} = r_{AB} \left(\frac{\kappa \mu_B}{\mu_A} \right)^{2/5} \tag{8}$$

The time of flight from periapsis to the SOI may be found through the true, hyperbolic, and mean anomalies. Denote this time of flight as Δ_{SOI}, which depends only upon the geometry of the hyperbolic flyby and the radius of the SOI.

For a flyby of target body i, it is now possible to obtain the SOI patch times with respect to the periapsis flyby time $t_{p,i}$. The patch times are given as t_i^- and t_i^+ in Eq. (9).

$$t_i^- = t_{p,i} - \Delta_{SOI} \qquad t_i^+ = t_{p,i} + \Delta_{SOI} \tag{9}$$

Intermediate states

The state of the ZSOI trajectory at the halfway point (in time) between each target body encounter is used as the intermediate state. The intermediate state at time $t_{inter,i}$ is propagated forward and backward in time to match the state at the patch points at t_i^+ and t_{i+1}^-. For an encounter of body i at t_i and of body $i+1$ at t_{i+1}, the intermediate state is found by Eq. (10).

$$t_{inter,i} = \frac{t_i + t_{i+1}}{2} \tag{10}$$

This time is a fixed parameter for each solution increment, and is not allowed to vary. Recall that the state of the spacecraft centered at the central body is known at each flyby time from the initial Lambert problem solution. That is, the spacecraft state $[\mathbf{r}_i, \mathbf{v}_i]$ is known with respect to the central body at encounter time t_i. This state is simply propagated forward in time from t_i to t_{inter} to determine the state $[\mathbf{r}_{inter}, \mathbf{v}_{inter}]$. For n target body encounters, there exist $n-1$ intermediate times, each with six defined state elements.

A schematic of the patch times with intermediate times for an example of three target bodies is given in Figure 4.

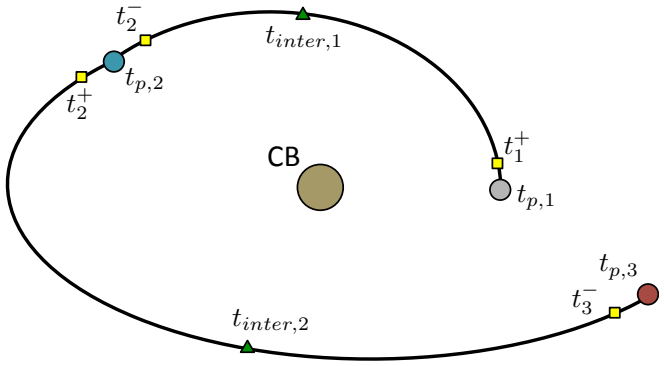

Figure 4: Patch times (squares) and intermediate times (triangles) for three target bodies

Parameters and constraints

It is now possible to fully define the parameters and constraints used in this approach to the inner loop solution. Qualitatively, the constraints are that the resulting trajectory must be continuous in position and velocity, and that the initial and final states with respect to the terminal bodies represent periapsis states.

The free time parameters are the n flyby periapsis times: $t_{p,1}$, $t_{p,2}$, ... , $t_{p,n}$. The intermediate times are fixed at the midpoint time between body encounters, found according to Eq. (10). Additionally, the patch times are fixed with respect to the body encounter time, according to Eq. (9). The encounter times are free, but the time Δ_{SOI} is fixed for each flyby.

The state at each non-terminal flyby body is represented by the state vectors $[\alpha_{p,2}, \beta_{p,2}, r_{p,2}, \mathbf{v}_{p,2}]$, ... ,$[\alpha_{p,n-1}, \beta_{p,n-1}, r_{p,n-1}, \mathbf{v}_{p,n-1}]$, where α and β are spherical angle parameters in the chosen reference frame. The state at the terminal bodies is given by α_1, β_1, $\mathbf{v}_{p,1}$, and α_n, β_n, $\mathbf{v}_{p,n}$, since the close approach distance at the terminal bodies is user-defined. Finally, the intermediate states

are represented by the position and velocity vectors $[\mathbf{r}_{inter,1}, \mathbf{v}_{inter,1}]$, ... , $[\mathbf{r}_{inter,n-1}, \mathbf{v}_{inter,n-1}]$. These parameters are all free to be varied by the optimization algorithm.

In all, there are n free time parameters, $6(n-2)$ full periapsis states elements, $6(n-1)$ intermediate state elements, and 10 total terminal body state elements. This yields a total of $13n-8$ state elements. Note that an initial guess must be obtained for the flyby parameters, which may be found by examining the flyby geometry of the velocity vectors from the Lambert targeting routine.

Constraints are separated into equality and inequality constraints. The equality constraints consist of the patch continuity constraints and the endpoint periapsis constraints, the latter of which are represented by a simple dot product, where $(\mathbf{r}_p \cdot \mathbf{v}_p) = 0$ must be satisfied in the body-centric frame. The inequality constraints ensure that time increases monotonically with each event, and that the periapsis altitude of the intermediate flybys is positive.

In all, there are $12(n-2)$ constraints at the non-terminal flyby bodies, 12 total constraints at the terminal bodies, and 2 terminal periapsis constraints, for a total of $12n-10$ equality constraints. There are $n-1$ intermediate times, $n-1$ flyby times after periapsis, $n-1$ flyby times before periapsis, n periapsis times, and $n-2$ flyby altitude constraints for a total of $5n-5$ inequality constraints.

It is worth noting that this problem may easily be cast as an optimization problem rather than a feasibility problem if there is a suitable cost parameter to be minimized. For example, if a spacecraft has finite-thrust arcs through the transfer legs of the tour, the relevant parameters and constraints may be included, and the cost function may be to minimize the amount of fuel used through the total mission.

Gradients

This implementation of this algorithm utilizes the well-known large-scale SQP optimization algorithm SNOPT[21] with no objective function to obtain a feasible solution to the trajectory continuity problem. Like many optimization methods, SNOPT requires the gradients of the constraints with respect to the parameters. These gradients are calculated using complex step differentiation, which is a novel method related to finite differencing based on perturbing the state parameters by a small complex term.[22]

CONTINUATION TO N-BODY DYNAMICS

Thus far, this algorithm consists of a method to converge a smooth, continuous trajectory between multiple bodies in a ZSOI model by using 1) an auxiliary Keplerian set of ephemerides, and 2) a zero-cost optimization model to solve the inner-loop feasibility problem. This procedure yields a continuous and differentiable solution in patched two-body dynamics, which is often not sufficiently accurate for high precision applications. A continuation method is now introduced to represent the converged state from the ZSOI model in an n-body ephemeris model.

The basic methodology behind this "outer loop" involves re-converging a feasible solution to the flyby/rendezvous problem in increasingly complex dynamical models while preserving flyby characteristics between each successive step. The re-convergence is implemented because it is easier to converge the intermediate models than it is to jump directly from a ZSOI guess to an n-body dynamical model. A control parameter $\kappa \in [0,1]$ is defined that controls the dynamics and ephemeris model used, with $\kappa = 0$ representing a purely ZSOI Keplerian model and $\kappa =$

1 representing an n-body ephemeris dynamical model. By incrementally increasing this control parameter, feasible solutions are calculated in models that approach the desired n-body dynamics.

The control parameter κ is tied to two important aspects of the model: body ephemeris and body mass (which relates to sphere of influence size). Although a more robust way to vary the ephemeris would be to calculate a new auxiliary ephemeris for every value of κ (for example, by numerically propagating body states according to the dynamics at the current value of κ), the ephemeris used for each value of κ is linearly related to the real and Keplerian ephemerides. In this manner, the endpoint values of κ (0 and 1) use the two exact ephemerides at the algorithm's disposal (Keplerian and real), and the values in between are an interpolation. The state of body B with respect to body A for each value of κ is calculated according to Eq. (1). This approach is similar to the methodology used by Lantoine and Russell for intermoon halo-to-halo transfers.[10]

A similar method is employed to vary the mass (and sphere of influence) of each body. There are two distinct regions in which the trajectory is calculated: around the central body (for transfers between target bodies) and about each target body for a departure, arrival, or flyby. In the ZSOI model, each target body is a point mass that instantaneously turns the trajectory. To approximate this turn, the flyby altitude must be very small for small values of κ, which corresponds to a small target body mass. Additionally, it is assumed that the effects of the central body are nonexistent for the "instantaneous" flyby of the ZSOI model. So, around each target body, the mass of each body is varied by κ. Around the central body, the mass of the central body does not change, but with increasing κ values, the target bodies exert an increasing gravitational force on the spacecraft. Therefore, the mass of the central body remains constant, while the mass of the target bodies is tied to κ. Eq. (11) summarizes the mass parameter values at each value of κ for the different regions that the spacecraft traverses.

$$\mu_{CB} = \begin{cases} \kappa \cdot \mu_{CB,final} & \text{if about target body} \\ \mu_{CB,final} & \text{if about central body} \end{cases} \qquad \mu_{TB} = \kappa \cdot \mu_{TB,final} \tag{11}$$

At any iteration in the continuation method, the equations of motion of the spacecraft about the central body are given by Eq. (12), where μ_{CB} and μ_{TB} are calculated according to Eq. (11). Note that $\mathbf{r}_{TB,i}$ is the i^{th} target body ephemeris position with respect to the central body.

$$\ddot{\mathbf{r}} = -\mu_{CB}\frac{\mathbf{r}}{r^3} - \sum_{i=1}^{n} \mu_{TB,i}\left(\frac{\mathbf{r}_{TB,i}}{r_{TB,i}^3} + \frac{\mathbf{r}-\mathbf{r}_{TB,i}}{|\mathbf{r}-\mathbf{r}_{TB,i}|^3}\right) \tag{12}$$

Similarly, the equations of motion of the spacecraft about any target body i are given by Eq. (13).

$$\mathbf{r}_{rel} = \mathbf{r}_{TB,j} - \mathbf{r}_{TB,i}$$
$$\ddot{\mathbf{r}} = -\mu_{TB,i}\frac{\mathbf{r}}{r^3} + \mu_{CB}\left(\frac{\mathbf{r}_{TB,i}}{r_{TB,i}^3} - \frac{\mathbf{r}+\mathbf{r}_{TB,i}}{|\mathbf{r}+\mathbf{r}_{TB,i}|^3}\right) - \sum_{j=1,j\neq i}^{n} \mu_{TB,j}\left(\frac{\mathbf{r}_{rel}}{|\mathbf{r}_{rel}|^3} + \frac{\mathbf{r}-\mathbf{r}_{rel}}{|\mathbf{r}-\mathbf{r}_{rel}|^3}\right) \tag{13}$$

A feasible solution is first found for $\kappa < 1$, which may be arbitrarily close to the ZSOI model. Once a solution has converged, κ is incremented to $\kappa_{i+1} = \kappa_i + \Delta\kappa$, where $\Delta\kappa$ is a constant step size defined by the user. Alternatively, a predictor-corrector scheme may be implemented to

dynamically change the step size, but a constant step size is assumed here. The converged states from the previous κ value are kept (other than the flyby periapsis states, which are altered to preserve flyby turning angles), and are assumed to represent a reasonable first guess to the feasible solution at this new value of the control parameter. This type of formulation is the computational basis for a mathematical treatise on general numerical continuation methods by Allgower and Georg,[23] and is similar to the continuation methods used in other works to determine families of trajectories.[13–17]

The patch times are changed in this process when κ is varied. Because the new value of κ leads to a change in the target body mass, according to Eq. (11), the estimate for the sphere of influence flight time Δ_{SOI} is altered for each target body.

Some care must be taken in how κ is incremented at each step. For a small number of target bodies or for short transfer times, it is best to begin κ at relatively large values to save computation time. In fact, for very simple problems (such as single body-to-body transfers with a small flight time), it may be possible to start with $\kappa = 1$. This scenario represents a case where the ZSOI converged solution is an acceptable guess to the n-body ephemeris model, which is an assumption that is often made by mission designers. The ability to add a control parameter generalizes this practice. Paffenroth, Doedel, and Dichmann[15] provide a concise mathematical and graphical depiction of the notion of the basin of attraction for κ. Large values of $\Delta\kappa$ may lead to a solution in a different family of tour trajectories, or may prevent the algorithm from converging at all.

EXAMPLES AND RESULTS

Ganymede to Callisto transfer

A simple example is converged with no intermediate body gravitational assist. A transfer from Ganymede to Callisto is presented to demonstrate the basic functionality of the algorithm. The initial value of κ is $\kappa_0 = 0.1$, and the constant step size is $\Delta\kappa = 0.1$. The converged solution was obtained with a CPU runtime of 3.5 seconds.

This particular trajectory does, in fact, converge using an initial value of $\kappa_0 = 1$ (i.e., a one-step convergence directly from the ZSOI guess). The non-unity κ_0 is used here simply to demonstrate the functionality of the continuation portion of the algorithm.

Figure 5 shows the final converged trajectory from Ganymede to Callisto about Jupiter as the central body. Figure 6 shows the body-centered flyby trajectories with values for the turning angles δ and the v_∞ magnitudes. The specified initial and final radius about Ganymede and Callisto is r_p = 3000 km for both bodies; this constant is not altered by the algorithm. The final converged encounter times are JD 2451921.998 for Ganymede departure and JD 2451926.008 for Callisto arrival.

Earth-Venus-Venus-Earth-Jupiter (EVVEJ) transfer

A more complex example involving five body encounters is chosen to demonstrate the utility of the algorithm as a whole. An initial ZSOI trajectory is obtained using EXPLORE, an in-house patched conics tour generating program external to the current work. A trajectory tour leaving Earth, flying twice by Venus and once by Earth, and arriving at Jupiter, is chosen as an initial ZSOI tour. This trajectory is quite complex, and it is difficult to obtain a converged solution directly from the initial guess with most optimizer packages.

After significant adjustment of the model parameters, the values $\kappa_0 = 0.02$ and $\Delta\kappa = 0.01$ were found to converge using the continuation algorithm. The specified initial and final radii about Earth

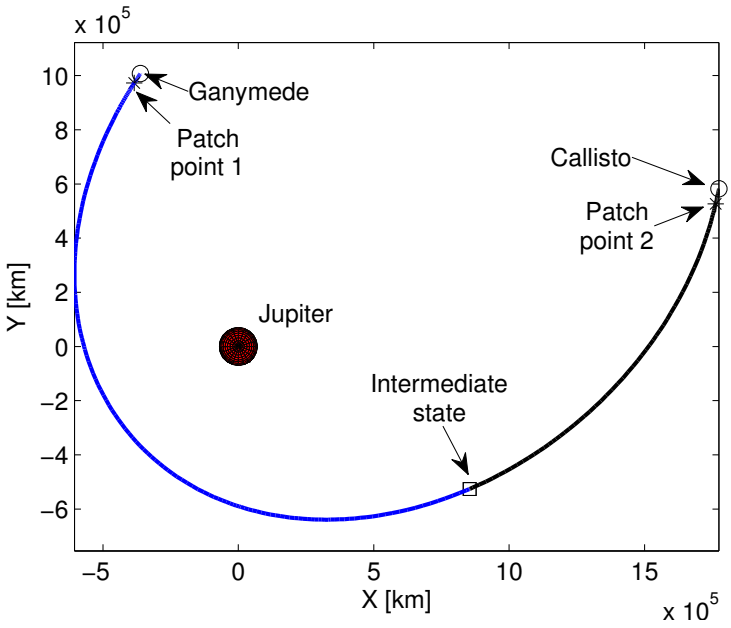

Figure 5: Converged transfer from Ganymede to Callisto

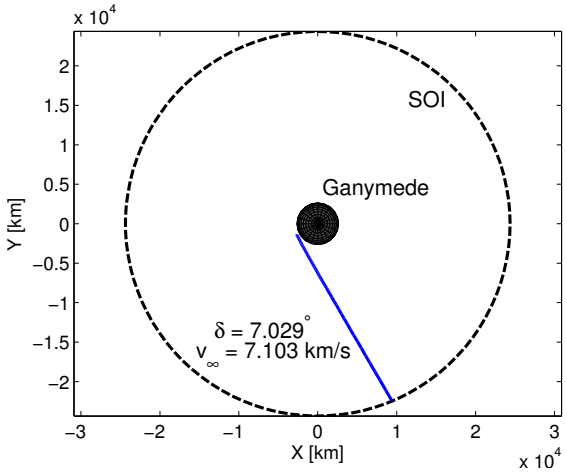

(a) Ganymede departure, specified r_p = 3000 km

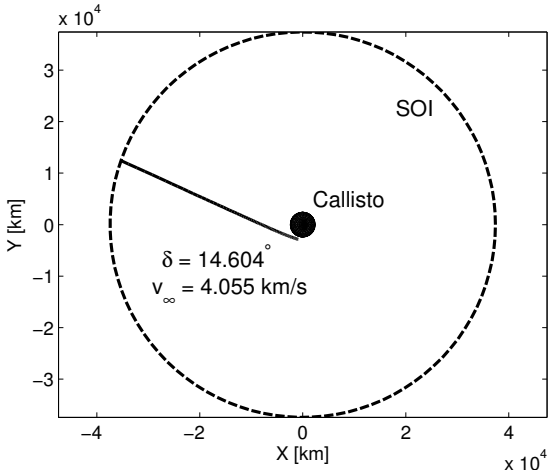

(b) Callisto arrival, specified r_p = 3000 km

Figure 6: Body-centered departure and arrival trajectories for Ganymede-Callisto transfer

and Jupiter are r_p = 10,000 km and r_p = 100,000 km, respectively; these constants are not altered by the algorithm. The converged solution was obtained with a CPU runtime of 2886.4 seconds, or about 48 minutes.

Figure 7 shows the final converged trajectory from Earth to Jupiter via two Venus flybys and an Earth flyby, with the Sun as the central body. Table 1 gives the relevant parameter results for the converged solution, including the flyby times and the states at Earth departure and Jupiter arrival.

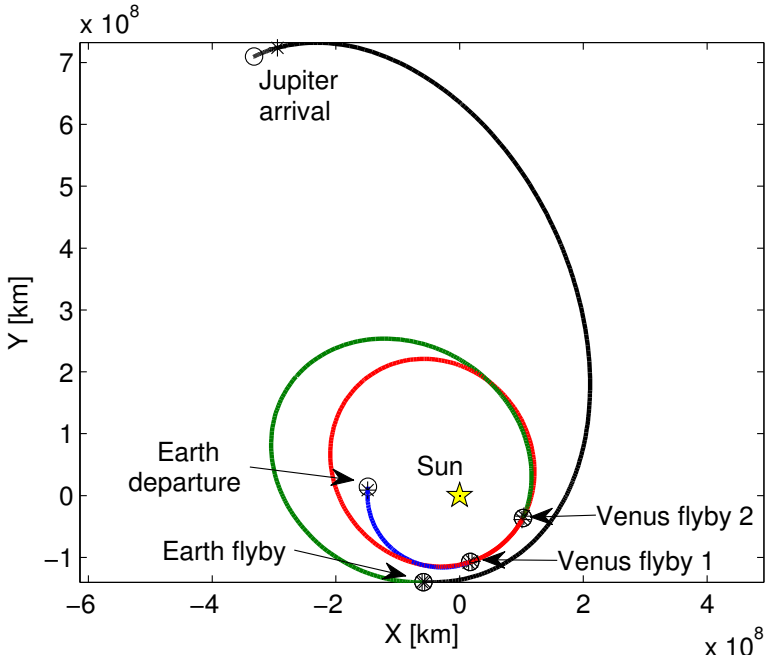

Figure 7: Converged EVVEJ transfer

Table 1: Converged parameters for EVVEJ transfer

Time	Value	Earth dep.	Value	Jupiter arr.	Value
t_0 [JD]	2458923.454	α_0 [deg]	-49.7	α_f [deg]	4.8
t_1 [JD]	2459020.514	β_0 [deg]	6.7	β_f [deg]	-5.0
t_2 [JD]	2459508.695	$v_{x,0}$ [km/s]	7.463	$v_{x,f}$ [km/s]	-3.233
t_3 [JD]	2460093.681	$v_{y,0}$ [km/s]	6.181	$v_{y,f}$ [km/s]	49.569
t_f [JD]	2461115.961	$v_{z,0}$ [km/s]	-1.024	$v_{z,f}$ [km/s]	9.865

Because of the more complex nature of the EVVEJ problem, the parameters vary more noticeably through the continuation process than they do in a simple body-to-body transfer. In particular, it is informative to see how relevant parameters vary throughout the continuation process, and to visualize how the flyby trajectories vary with different values of the control parameter κ.

Figure 8 shows the variation of the departure and arrival times from their initial guess through the continuation process. The intermediate flyby times do not vary significantly from their initial values, and are not shown in this figure. The initial and final times vary sharply at the beginning (low values of κ), but become more continuous for higher values of κ. The smooth nature of the encounter time variation past $\kappa = 0.1$ suggests that the value of $\Delta\kappa$ may benefit from being carefully increased when the values vary less significantly with each change in κ.

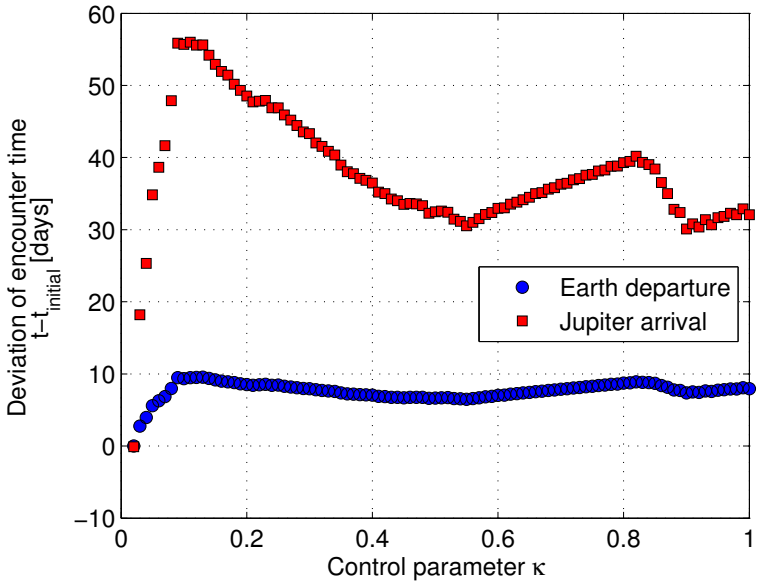

Figure 8: Variation of encounter times

Figure 9 depicts the flyby altitude variation through the continuation process. Because the initial and final radii (about Earth and Jupiter, respectively) are both specified to be constant, these radii are not shown here. At the final converged solution, all flybys exhibit positive flyby altitudes.

Figure 10 shows all iterations of the first flyby trajectory at Venus in a Venus-centered inertial frame. As κ is increased, the periapsis of the flyby increases between successive iterations. The final converged value for the flyby periapsis radius is greater than the radius of Venus, so the flyby is feasible with given physical parameters.

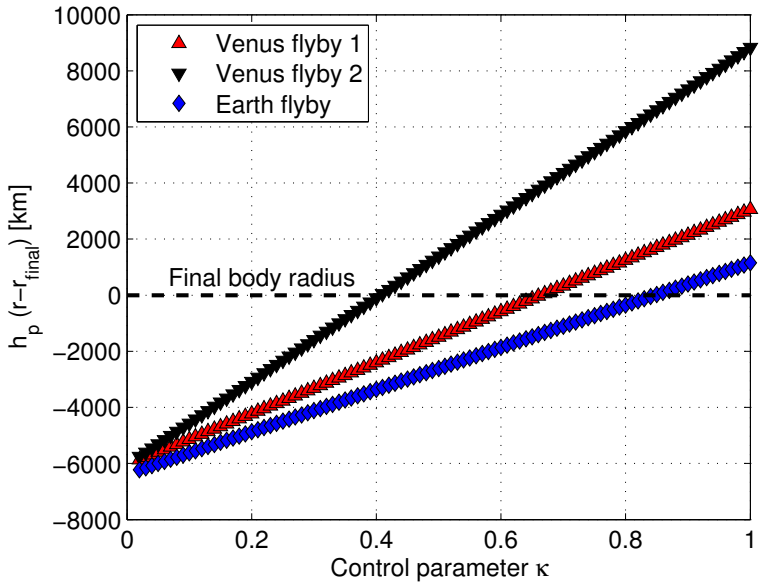

Figure 9: Variation of flyby altitudes

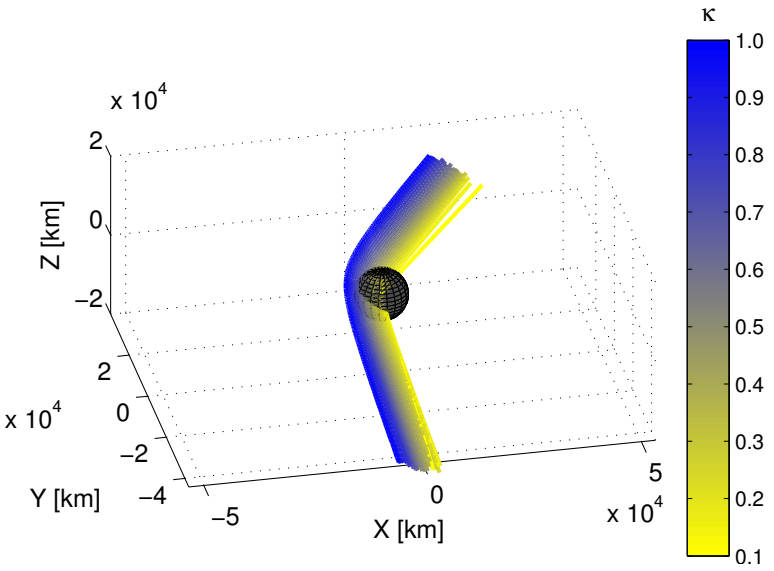

Figure 10: Successive iterations of the first flyby trajectory at Venus. Venus is shown at its final (actual) radius.

CONCLUSION

In designing tour missions to planets or moons, mission designers often begin with a zero sphere of influence (ZSOI) model, or other simplistic dynamical model. To obtain a trajectory in true dynamics, however, the simplistic trajectory must be transferred to an n-body ephemeris model that takes body gravitational effects into account. The procedure to link the trajectory between the two models is often assumed to be trivial, or it is assumed that the ZSOI model represents a suitable initial guess for convergence in the n-body model. This assumption is often invalid, especially for complex flyby profiles and fast-changing dynamics.

A multi-part method is presented here to take a ZSOI initial guess and converge a trajectory in an n-body ephemeris model. This approach uses a continuation method, where a control parameter κ is tied to body mass, ephemeris, and sphere of influence size. Turning angles and flyby properties are preserved through the continuation process, ensuring that the final converged trajectory is qualitatively similar to the original ZSOI trajectory. Target body flyby parameters are defined from the simplified model, and an auxiliary Keplerian ephemeris is introduced to facilitate the calculation of "fake" ephemerides at each step in the continuation process. This method has applications in designing trajectories to outer planets and in small-body tour design, where simplified dynamics are usually not an acceptable one-step initial guess for converging an n-body ephemeris trajectory.

ACKNOWLEDGMENT

This work was supported in part by a NASA Research Announcement/Research Opportunities in Space and Earth Sciences award (no. NNX13AH04G).

REFERENCES

[1] N. J. Strange and J. M. Longuski, "Graphical Method for Gravity-Assist Trajectory Design," *Journal of Spacecraft and Rockets*, Vol. 39, Jan. 2002, pp. 9–16, 10.2514/2.3800.

[2] D. Izzo, L. F. Simões, M. Märtens, G. C. d. Croon, A. Heritier, and C. H. Yam, "Search for a Grand Tour of the Jupiter Galilean Moons," *Proceeding of the 15th Annual conference on Genetic and evolutionary computation conference - GECCO '13*, New York, New York, USA, ACM Press, 2013, pp. 1301–1308, 10.1145/2463372.2463524.

[3] C. M. Spreen, M. J. Mueterthies, K. W. Kloster, and J. M. Longuski, "Preliminary Analysis of Ballistic Trajectories to Uranus Using Gravity-Assists from Venus, Earth, Mars, Jupiter, and Saturn," *Proceedings of the AAS/AIAA Astrodynamics Specialist Conference*, 2011, pp. 3411–3428.

[4] R. S. Wilson and K. C. Howell, "Trajectory Design in the Sun Earth Moon System Using Lunar Gravity Assists," *Journal of Spacecraft and Rockets*, Vol. 35, No. 2, 1998, pp. 191–198.

[5] D. V. Byrnes and H. L. Hooper, "Multi-Conic: A Fast and Accurate Method of Computing Space Flight Trajectories," *AAS/AIAA Astrodynamics Conference*, 1970. AIAA Paper 70–1062.

[6] B. G. Marchand, K. C. Howell, and R. S. Wilson, "Improved Corrections Process for Constrained Trajectory Design in the n-Body Problem," *Journal of Spacecraft and Rockets*, Vol. 44, July 2007, pp. 884–897, 10.2514/1.27205.

[7] B. Buffington and N. Strange, "Patched-Integrated Gravity-Assist Trajectory Design," *AIAA/AAS Astrodynamics Specialist Conference*, 2007, pp. 403–422.

[8] P. R. Griesemer, C. Ocampo, and D. S. Cooley, "Targeting Ballistic Lunar Capture Trajectories Using Periodic Orbits," *Journal of Guidance, Control, and Dynamics*, Vol. 34, May 2011, pp. 893–902, 10.2514/1.46843.

[9] G. Picot, "Shooting and numerical continuation methods for computing time-minimal and energy-minimal trajectories in the Earth-Moon system using low propulsion," *Discrete and Continuous Dynamical Systems - Series B*, Vol. 17, Oct. 2011, pp. 245–269, 10.3934/dcdsb.2012.17.245.

[10] G. Lantoine and R. P. Russell, "Near Ballistic Halo-to-Halo Transfers between Planetary Moons," *Journal of the Astronautical Sciences*, Vol. 58, No. 3, 2011, pp. 335–363.

[11] R. P. Russell and N. J. Strange, "Cycler Trajectories in Planetary Moon Systems," *Journal of Guidance, Control, and Dynamics*, Vol. 32, Jan. 2009, pp. 143–157, 10.2514/1.36610.

[12] R. P. Russell and C. A. Ocampo, "Optimization of a Broad Class of Ephemeris Model Earth-Mars Cyclers," *Journal of Guidance, Control, and Dynamics*, Vol. 29, Mar. 2006, pp. 354–367, 10.2514/1.13652.

[13] J. D. Biggs and C. McInnes, "Solar Sail Formation Flying for Deep-Space Remote Sensing," *Journal of Spacecraft and Rockets*, Vol. 46, May 2009, pp. 670–678, 10.2514/1.42404.

[14] C. C. Chow and B. F. Villac, "Mapping Autonomous Constellation Design Spaces Using Numerical Continuation," *Journal of Guidance, Control, and Dynamics*, Vol. 35, Sept. 2012, pp. 1426–1434, 10.2514/1.56434.

[15] R. C. Paffenroth, E. J. Doedel, and D. J. Dichmann, "Continuation of Periodic Orbits Around Lagrange Points and AUTO2000," *Advances in the Astronautical Sciences*, 2001, pp. 41–60.

[16] K. Yagasaki, "Computation of low energy Earth-to-Moon transfers with moderate flight time," *Physica D: Nonlinear Phenomena*, Vol. 197, Oct. 2004, pp. 313–331, 10.1016/j.physd.2004.07.005.

[17] J. Casoliva, J. M. Mondelo, B. F. Villac, K. D. Mease, E. Barrabes, and M. Olle, "Two Classes of Cycler Trajectories in the Earth-Moon System," *Journal of Guidance, Control, and Dynamics*, Vol. 33, Sept. 2010, pp. 1623–1640, 10.2514/1.46856.

[18] B. Tapley, B. Schutz, and G. Born, *Statistical Orbit Determination*. Burlington, MA: Elsevier, 2004.

[19] R. Battin, *An Introduction to the Mathematics and Methods of Astrodynamics, Revised ed.* Reston, VA: American Institute of Aeronautics and Astronautics, 1999.

[20] D. Vallado, *Fundamentals of Astrodynamics and Applications, Third ed.* New York, NY: Springer, 2007.

[21] P. E. Gill, W. Murray, and M. a. Saunders, "SNOPT: An SQP Algorithm for Large-Scale Constrained Optimization," *SIAM Journal on Optimization*, Vol. 12, Jan. 2002, pp. 979–1006, 10.1137/S1052623499350013.

[22] J. R. R. A. Martins, P. Sturdza, and J. J. Alonso, "The Complex-Step Derivative Approximation," *ACM Transactions on Mathematical Software*, Vol. 29, No. 3, 2003, pp. 245–262.

[23] E. L. Allgower and K. Georg, *Numerical Continuation Methods: An Introduction*. New York: Springer, 1990.